

# Finite-Temperature Instantons from First Principles

Thomas Steingasser,<sup>1,2,\*</sup> Morgane König,<sup>1,†</sup> and David I. Kaiser<sup>1,‡</sup>

<sup>1</sup>*Department of Physics, Massachusetts Institute of Technology, Cambridge, MA 02139, USA*

<sup>2</sup>*Black Hole Initiative at Harvard University, 20 Garden Street, Cambridge, MA 02138, USA*

(Dated: February 21, 2024)

We derive the finite-temperature quantum-tunneling rate from first principles. The rate depends on both real- and imaginary-time; we demonstrate that the relevant instantons should therefore be defined on a Schwinger-Keldysh contour, and how the familiar Euclidean-time result arises from it in the limit of large physical times. We generalize previous results for general initial states, and identify distinct behavior in the high- and low-temperature limits, incorporating effects from background fields. We construct a consistent perturbative scheme that incorporates large finite-temperature effects.

**Introduction.** Quantum tunneling is arguably one of the most important examples of non-perturbative quantum phenomena [1–6]. Despite recent advances in our understanding of this process [7–28], many of its aspects remain elusive, in particular when tunneling out of non-vacuum states is concerned, e.g., for finite temperatures.

Based on analogies with the zero-temperature limit and the rigorously derived decay-rate formula for classical systems, the decay rate  $\Gamma$  per spatial volume  $V$  of a false vacuum at finite temperature has long been conjectured to be given by the imaginary part of the system’s free energy  $F$  [5, 6] as

$$\frac{\Gamma}{V} \simeq -2 \operatorname{Im}(F) = -2 \operatorname{Im} \left( -T \log \int_{\varphi(0)=\varphi(\beta)} \mathcal{D}\varphi e^{-S_E[\varphi]} \right). \quad (1)$$

Here, and throughout the remainder of this article,  $\beta = T^{-1}$  denotes the inverse temperature. Eq. (1) can be understood as imposing periodic boundary conditions along the Euclidean-time axis on the zero-temperature result derived in Ref. [3]. Alternatively, one may note that this formula appears to reproduce the more rigorously derived decay rate for classical systems in the high-temperature limit [29–33], given that the relevant fields have large occupation numbers [34–37].

A series of recent articles, however, has pointed out that the zero-temperature formula motivating this expression is plagued by several conceptual issues, which seem to require multiple nontrivial modifications to the standard procedure if the well-established, leading-order result is to be recovered [7–9]. Most important, the imaginary part of the bounce contribution to the path integral in Eq. (1) is canceled by contributions from other saddle points, leading to a vanishing decay rate. Whereas these can be dealt with by artificially restricting the domain of the path integral through the so-called *potential deformation method*, the only motivation to do so is to recover

Coleman’s famous leading-order result [8]. Because these cancellations do not depend on the size of the Euclidean time interval of interest, it is straightforward to see that the finite-temperature result inherits these issues.

A more subtle problem of this approach is the role of time-dependence. It is well-understood that the decay rate is *a priori* a real-time-dependent observable [7, 8]. In the zero-temperature case, the Euclidean time-dependence arises only through a Wick rotation, and the apparent time-independence through the limit of large times relative to the natural time-scale of the system in which the decay occurs. This is however fundamentally different from the ansatz of Eq. (1), in which the Euclidean time-dependence is a manifestation of the system’s thermal probability distribution. From this perspective, one would expect the finite-temperature decay rate to have both a Euclidean- and real-time dependence, while the latter is absent in Eq. (1). Yet this seems to be in tension with the requirement to recover the classical result in the high-temperature limit, as it is not immediately evident how the latter suppresses the real-time dependence.

A similar conclusion can be reached from a different perspective. The finite-temperature field can be understood as a mixture of excited states. This has motivated the suggestion to obtain the total decay rate by calculating the rate for each of these states individually, and then performing a sum over each state within the ensemble [38, 39]. As each of the individual decay rates is independent of the occupational probability of the other states within the ensemble, each rate should be determined entirely by a real-time calculation, corresponding to different Euclidean times. How this leads to a quantity defined on a single Euclidean-time interval, however, remains far from clear for a general system.

**The Decay Rate from First Principles.** To address these problems, we derive an expression for the decay rate from first principles, which can be defined through the change of probability that the field can be found within a region of interest. This approach has been used to derive the decay rate at zero temperature in Refs. [7, 8], and various attempts to generalize it have been made in Refs. [10–12, 40, 41]. Following Ref. [41], we describe the system through its density matrix  $\rho$ . The

\* [tstngssr@mit.edu](mailto:tstngssr@mit.edu)

† [mkonig@mit.edu](mailto:mkonig@mit.edu)

‡ [dikaiser@mit.edu](mailto:dikaiser@mit.edu)



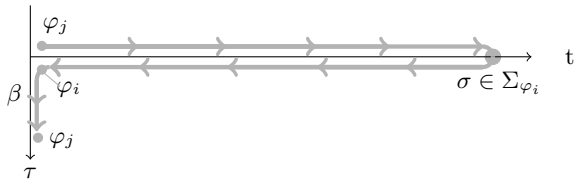


FIG. 2. The Schwinger-Keldysh contour arising from the microphysical picture. The horizontal contours represent the decay rate out of the initial state  $\varphi_i$  as obtained through the real-time computation developed in Ref. [10]. The vertical contour represents the occupation probability of this initial state, which itself depends on the temperature  $T = \beta^{-1}$ . As usual, the integral over the boundary condition  $\varphi_j$  implies periodicity in direction of imaginary-time  $\tau$  with period  $\beta$ .

symmetry of the system suggests that the dominant contribution to the decay rate arises from the case  $\varphi_i = \varphi_j$ . Thus, the contribution from the contour along the real-time axis can be understood as the tunneling rate out of the initial state  $\varphi_i$ , as described in Ref. [10]. The factor  $\rho_{ij}$ , meanwhile, can be understood as the occupational probability of this initial state within the thermal ensemble.

Whereas this establishes a consistent way to define the decay rate as a Schwinger-Keldysh process, evaluating Eq. (7) still remains generally impractical due to the complexity of the saddle-point equations for arbitrary temperatures [38, 39].

*Thermodynamical picture.* In order to evaluate Eq. (3), we rewrite the probability of Eq. (2) by inserting a decomposition of unity in terms of field eigenstates and make the substitution  $\beta = \beta_1 + \beta_2$ ,

$$\begin{aligned} \mathcal{P}_{\mathcal{R}} &= \int_{\mathcal{R}} \mathcal{D}\varphi_f \langle \varphi_f | e^{iHt} \rho e^{-iHt} | \varphi_f \rangle \\ &= \int_{\mathcal{R}} \mathcal{D}\varphi_f \langle \varphi_f | e^{iHt} e^{-H\beta_1} e^{-H\beta_2} e^{-iHt} | \varphi_f \rangle \\ &= \int_{\mathcal{F}} \mathcal{D}\varphi_* \int_{\mathcal{R}} \mathcal{D}\varphi_f \langle \varphi_f | e^{iHt(1+i\frac{\beta_1}{t})} | \varphi_* \rangle \langle \varphi_* | e^{-iHt(1-i\frac{\beta_2}{t})} | \varphi_f \rangle. \end{aligned} \quad (9)$$

In the limit of large physical times, the temperature-dependent term acts as a regulator of the time evolution operators,  $\epsilon_{1,2} = \beta_{1,2}/t$ . In terms of complex-time contours, this amounts to picking two paths with  $\Delta\tau_{1,2} = \beta_{1,2}$ , see Fig. 3. For  $\beta_1 = \beta_2$ , the contribution of each  $\varphi_*$  can be identified with the decay rate out of the corresponding eigenstate as derived in Ref. [10], up to the difference in the normalization factor  $Z_\beta$ . It is now straightforward to adapt the calculations of Refs. [7, 8, 10], lead-

ing to

$$\begin{aligned} \Gamma &= \frac{1}{Z_\beta} \int_{\mathcal{F}} \mathcal{D}\varphi_* \int_{\Sigma_{\varphi_j}} \mathcal{D}\sigma \bar{D}_F^{\epsilon_1}(\varphi_* | \sigma, t) D_F^{\epsilon_2}(\sigma, t | \varphi_*) + c.c. \\ &= \frac{1}{Z_\beta} \int_{\mathcal{F}} \mathcal{D}\varphi_* \int_{\Sigma_{\varphi_*}} \int_{\varphi_1(0)=\varphi_*}^{\varphi_1(t)=\sigma} \mathcal{D}\sigma \int \mathcal{D}\varphi_1 e^{iS_{\epsilon_1}[\varphi_1]} \delta(F_{\varphi_*}[\varphi_1] - t) \\ &\quad \times \left( \int_{\varphi_2(0)=\varphi_*}^{\varphi_2(t)=\sigma} \mathcal{D}\varphi_2 e^{iS_{\epsilon_2}[\varphi_2]} \right)^* + c.c. \end{aligned} \quad (10)$$

Here, all quantities with a label  $\epsilon_{1,2}$  are to be understood as regularized using the parameter  $\epsilon_{1,2} = \beta_{1,2}/t$ .

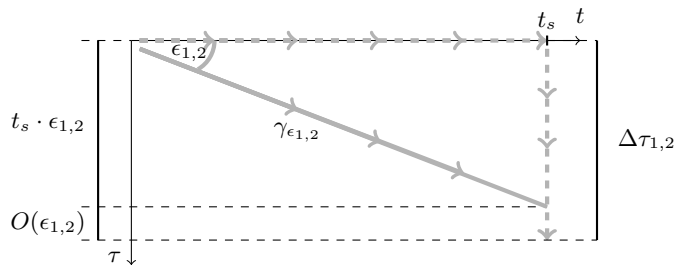


FIG. 3. The exponent of the decay rate arises from the integral of the stationary-phase solution's complex Lagrange function over the diagonal time contour  $\gamma_{\epsilon_{1,2}}$ . This contour can be deformed into pieces along the real- and imaginary-time axis, respectively. Here,  $\tau$  denotes the imaginary time obtained through the usual Wick rotation. The length of the imaginary-time piece coincides with that of the instanton's imaginary-time support,  $\Delta\tau_{1/2}$ , up to a factor of order of the regularization parameter  $\epsilon$ . The time  $t_s$  is chosen such that the stationary-phase solution satisfies the desired boundary conditions up to deviations of order  $\epsilon$ .

Eq. (10) can be evaluated through a stationary phase approximation following the technique discussed in Ref. [10]. First, the normalization factor  $Z_\beta$  is dominated by the constant saddle point  $\varphi_{FV}$ . Demanding the potential to vanish in the false vacuum, this leads to a vanishing exponent. The numerator meanwhile is, to leading order, determined by solutions  $\bar{\phi}_{1,2}$  of the equations of motion along the complex-time contours  $\gamma_{\epsilon_{1,2}}$  shown in Fig. 3 and their corresponding actions,

$$S_1 \equiv S[\bar{\phi}_1], \quad S_2 \equiv S[\bar{\phi}_2]. \quad (11)$$

This amounts to

$$\begin{aligned} \Gamma &= A \cdot e^{iS_1 - iS_2^*} \\ &= A \cdot e^{i(\text{Re}[S_1] - \text{Re}[S_2]) - (\text{Im}[S_1] + \text{Im}[S_2])}, \end{aligned} \quad (12)$$

with some loop-coefficient  $A$ .

The integrals over the boundary values  $\varphi_*$  and  $\sigma$  together with the arbitrariness in the partition of  $\beta$  imply periodic boundary conditions along the imaginary-time axis. A first analysis of such solutions has recently

been given in Ref. [10], where they were dubbed (*periodic steadyons*). Importantly, these solutions can be expected to satisfy the relevant boundary conditions,  $\text{Re}(\bar{\phi}(t_s)) \simeq \sigma \in \Sigma_{\varphi_*}$  and  $\text{Im}(\bar{\phi}(t_s)) \simeq 0$ , only for a countable number of physical times  $t_s$ . These times are multiples of the duration of the periodic motion  $\varphi_* \rightarrow \varphi_*$  in real time. This is, however, sufficient to obtain a well-defined decay rate in the limit  $t \rightarrow \infty$ .

Due to the appearance of complex time in their equations of motion, the steadyons are themselves complex-valued, as are their corresponding actions  $S_{1,2}$  [18–24, 26, 28]. For the special case  $\epsilon_1 = \epsilon_2$ , it is argued in Ref. [10] that the sum of these actions reproduces the Euclidean action of their corresponding instanton in the relevant limit  $t \rightarrow \infty$ .

This argument can be generalized to the case at hand as follows. First, we deform the diagonal paths  $\gamma_{\epsilon_{1,2}}$  into components along the real- and imaginary-time axis, respectively. See Fig. 3. The actions along the real-time axis are strictly real and, naturally, independent of  $\epsilon$ . Thus, the contributions of the actions' real parts to the decay rate in Eq. (12) cancel. Along the contour parallel to the imaginary-time axis, the steadyons reproduce their corresponding instanton solutions in the limit  $t \rightarrow \infty$ . Together with the additional factor of  $i$  from the direction of the contour, this implies that, in this limit, the imaginary parts of  $S_{1,2}$  reproduce the Euclidean actions of the instantons corresponding to the respective steadyons.

The relation between steadyon and instanton is illustrated in Fig. 4 for the simple example of a point particle in the double-well potential  $V(x) = \frac{1}{4}(x^2 - 1)^2$ .

To better understand the analogy between the tunneling rate in the thermodynamical picture and for a pure, excited state, we may first note that the Euclidean action of any periodic instanton with period  $\beta$  satisfies  $S_E = E\beta + W$ , where  $E$  is the energy of the initial state and  $W$  is the usual WKB exponent [42]. For the thermal ensemble, where  $Z_\beta$  is dominated to leading order by the contribution from the constant saddle point with  $S_E = 0$ , this result has a simple interpretation as the superposition of a thermal suppression (first term) and a tunneling suppression (second term).

The finite-temperature result differs from that for a pure state through the periodic boundary condition. In Ref. [10], it is shown that the normalization factor for a pure state is dominated by a non-trivial stationary phase solution leading to an enhanced rate, counteracting the thermal suppression factor. For the numerator of the rate, dropping the periodicity allows for a wider class of stationary-phase solutions, further enhancing the decay rate.

**Multifield Models and the Effective Action.** In many real-world applications, including the stability of the Higgs vacuum in the Standard Model (SM), one has to take into account the effects of external degrees of freedom, which affect the tunneling only through interactions. We can incorporate them into our definition of

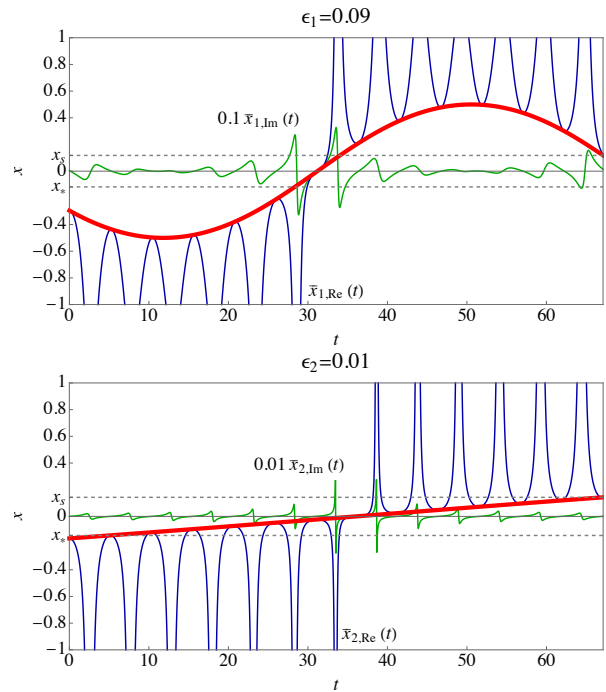


FIG. 4. The periodic steadyons for a point particle in a double-well potential with the partition  $\beta_1 = 0.9\beta$ ,  $\beta_2 = 0.1\beta$ . The blue curves represent the real part of the complex steadyon, the green curves its imaginary part. The projection of the steadyon on the complex-time contour parallel to the imaginary-time axis, represented by the red curve, reproduces the familiar instanton. The time  $t_s$  is a multiple of the period of the real-part's driven oscillatory motion.

the tunneling process by extending the trace as

$$\mathcal{P}_{\mathcal{R}}(t) = \int \mathcal{D}\chi \int_{\mathcal{R}} \mathcal{D}\varphi \langle \varphi, \chi, t | \rho | \varphi, \chi, t \rangle. \quad (13)$$

This amounts to allowing for any configuration of the background fields  $\chi$  after the tunneling. For the zero-temperature case, it was argued in Ref. [8] that the proper way to account for these additional path integrals is to first solve for the instanton using the tree-level potential and only afterwards integrate over the remaining fields, such that their effect is reduced to additional contributions to the prefactor  $A$ .

It is well-known that loop-corrections to the potential can be significant in finite-temperature systems, e.g., through particles obtaining thermal masses [43–45]. This suggests to integrate out the external fields *before* performing the saddle-point approximation in order to capture these effects, which would amount to working with an effective action. In Ref. [8], however, it was pointed out that the instanton background can spoil the convergence of momentum-dependent corrections to the effective action. Denoting the field giving rise to the instanton by  $\phi$ , these are suppressed by increasingly higher orders of  $m_\phi^2/m_i^2$ , where  $m_i^2$  is the field-dependent mass of the particles being integrated out [45–47]. Hence, while the

fluctuations of the field  $\phi$  always need to be evaluated in their functional determinant form, any other field can be accounted for through its contributions to the effective action as long as its (effective) mass is larger than that of the scalar field around the instanton [48]. An important example for this scenario is thermally induced electroweak vacuum decay in the SM. Combining the scaling of the instanton,  $\phi \sim |\lambda|^{-1/2}T$ , with the inferred values of the relevant couplings at high energies, it is straightforward to find that all particles besides the Higgs itself and the Goldstone modes can be integrated out consistently. Here,  $\lambda$  denotes the Higgs field's quartic self-coupling.

**Important Limits.** In the limit of low temperatures our approach naturally reproduces the familiar zero-temperature results as  $\beta \rightarrow \infty$ . As the high-temperature limit corresponds to large occupation numbers, it can, in general, be expected to yield the classical limit [29–37], in which the exponent is to leading order determined by a constant solution in the Euclidean-time direction.

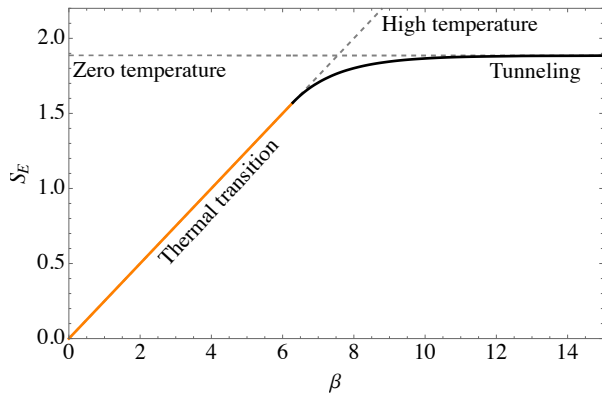


FIG. 5. The Euclidean action as a function of inverse temperature  $\beta$  for the potential  $V(x) = \frac{1}{4}(x^2 - 1)^2$ . We find a smooth limit for both high and low temperatures. Quantum tunneling is only relevant for  $\beta \gtrsim 6.28$  in these units, which corresponds to the oscillator period for motions around the minimum of the inverted potential. For smaller values of  $\beta$ , the transition is entirely determined by thermal excitations.

For a point particle, the instanton can be represented as a periodic motion in the inverse potential. It is easy to see that, for a generic potential, the Euclidean time necessary for such motions is bounded from below by some  $\Delta\tau_{\min}$  that scales with the mass scale of the potential. Hence, for smaller values of  $\beta$  no periodic solution exists, leaving only the saddle point corresponding to the particle being at rest on top of the potential barrier,  $\bar{\phi} = \varphi_{\text{top}}$ . It is worth noting that this configuration on its own violates the crossing condition. This changes, however, once fluctuations around it are taken into account, as the path integral over all configurations also covers a non-vanishing subset for which  $\delta\phi < 0$  until the crossing time.

The transition between the instanton-dominated regime to the sphaleron-dominated regime is easily understood through the relation  $S_E = \beta E + W$ . For a

generic potential, the smallest possible value of  $\beta$  corresponds to infinitesimally small oscillations around  $\varphi_{\text{top}}$ . This implies immediately that in this limit  $W \rightarrow 0$  and  $E \rightarrow E[\varphi_{\text{top}}]$ , suggesting a smooth limit. The properties of this limit are investigated in more detail in Ref. [49].

An important subtlety is that this limit can be prevented by background-field effects. Integrating out heavy degrees of freedom at a finite temperature induces temperature-dependent corrections to the potential, including a mass term. For temperatures significantly larger than the tree-level mass, the magnitude of these terms is controlled by the temperature alone. As an example, the thermal mass is generally of the form  $m_T^2 = \kappa \cdot T^2$ , with some combination of the scalar field's couplings to the background fields  $\kappa$ , but, importantly, no additional loop-suppression factor  $(4\pi)^{-2N_{\text{loop}}}$ . In other words, all relevant energy scales of the theory are of order of the temperature up to numerical coefficients, which can be  $\mathcal{O}(1)$  for sufficiently large couplings. This can be understood as the energy per particle increasing due to its coupling to an increasingly hot background plasma counteracting the increase in the occupation number. An important example for this behavior is the SM Higgs field, for which we find that the coefficient  $\kappa$  lies within the range 0.1 – 0.2 for all energies above the central value of the instability scale,  $\mu_I \sim 10^{11}$  GeV [50]. While this establishes in principle the possibility of a perturbative expansion, it also suggests that precision calculations should take into account leading-order corrections in  $\kappa$ , in particular since the effects of, e.g., potentially large neutrino Yukawa couplings can further enhance this effect [12].

**Discussion.** We have derived compact path-integral representations for the tunneling rate for an arbitrary finite-temperature system. Unlike previous treatments, which have often relied on analogies, our first-principles derivation clarifies several conceptual questions. In particular, we have shown that the finite-temperature decay rate can indeed be understood as a superposition of contributions from each state in the thermal ensemble. This expression can be rewritten in a way that allows one to perform a combined saddle-point approximation. The properties of the resulting complex-time instanton imply that, in the limit of large physical times, the exponent of the decay rate converges to the Euclidean action of the familiar Euclidean-time instanton with period  $\beta$ .

This simple relation explains how the decay rate, which is *a priori* a real-time-dependent quantity, can be described in terms of a Euclidean-time quantity. This result can be understood as the tunneling being dominated by the contribution of one state in the thermal ensemble. In addition, we have analyzed the influence of background fields on the decay rate as well as subtleties related to both the high- and low-temperature limits. This establishes a robust foundation for tunneling and bubble-nucleation calculations at arbitrary temperatures.

*Acknowledgements.* TS's contributions to this work

were made possible by the Walter Benjamin Programme of the Deutsche Forschungsgemeinschaft (DFG, German Research Foundation) – 512630918. MK is supported in part by the MLK Visiting Scholars Program at MIT. Portions of this work were conducted in MIT’s Center for Theoretical Physics and partially supported by the U.S. Department of Energy under Contract No. DE-

SC0012567. This project was also supported in part by the Black Hole Initiative at Harvard University, with support from the Gordon and Betty Moore Foundation and the John Templeton Foundation. The opinions expressed in this publication are those of the author(s) and do not necessarily reflect the views of these Foundations.

- 
- [1] I. Y. Kobzarev, L. B. Okun, and M. B. Voloshin, Bubbles in Metastable Vacuum, *Yad. Fiz.* **20**, 1229 (1974).
- [2] S. R. Coleman, The Fate of the False Vacuum. 1. Semi-classical Theory, *Phys. Rev. D* **15**, 2929 (1977), [Erratum: *Phys.Rev.D* 16, 1248 (1977)].
- [3] C. G. Callan, Jr. and S. R. Coleman, The Fate of the False Vacuum. 2. First Quantum Corrections, *Phys. Rev. D* **16**, 1762 (1977).
- [4] F. Devoto, S. Devoto, L. Di Luzio, and G. Ridolfi, False vacuum decay: an introductory review, *J. Phys. G* **49**, 103001 (2022), [arXiv:2205.03140 \[hep-ph\]](#).
- [5] A. D. Linde, Fate of the False Vacuum at Finite Temperature: Theory and Applications, *Phys. Lett. B* **100**, 37 (1981).
- [6] A. D. Linde, Decay of the False Vacuum at Finite Temperature, *Nucl. Phys. B* **216**, 421 (1983), [Erratum: *Nucl.Phys.B* 223, 544 (1983)].
- [7] A. Andreassen, D. Farhi, W. Frost, and M. D. Schwartz, Direct Approach to Quantum Tunneling, *Phys. Rev. Lett.* **117**, 231601 (2016), [arXiv:1602.01102 \[hep-th\]](#).
- [8] A. Andreassen, D. Farhi, W. Frost, and M. D. Schwartz, Precision decay rate calculations in quantum field theory, *Phys. Rev. D* **95**, 085011 (2017), [arXiv:1604.06090 \[hep-th\]](#).
- [9] A. Andreassen, W. Frost, and M. D. Schwartz, Scale Invariant Instantons and the Complete Lifetime of the Standard Model, *Phys. Rev. D* **97**, 056006 (2018), [arXiv:1707.08124 \[hep-ph\]](#).
- [10] T. Steingasser and D. I. Kaiser, Quantum tunneling from excited states: Recovering imaginary-time instantons from a real-time analysis, (2024), [arXiv:2402.00099 \[hep-th\]](#).
- [11] T. Steingasser, *New perspectives on solitons and instantons in the Standard Model and beyond*, *Ph.D. thesis*, Munich U. (2022).
- [12] G. Chauhan and T. Steingasser, Gravity-improved metastability bounds for the Type-I seesaw mechanism, *JHEP* **09**, 151, [arXiv:2304.08542 \[hep-ph\]](#).
- [13] J. R. Espinosa, A Fresh Look at the Calculation of Tunneling Actions, *JCAP* **07**, 036, [arXiv:1805.03680 \[hep-th\]](#).
- [14] J. R. Espinosa, Fresh look at the calculation of tunneling actions including gravitational effects, *Phys. Rev. D* **100**, 104007 (2019), [arXiv:1808.00420 \[hep-th\]](#).
- [15] J. R. Espinosa and T. Konstandin, A Fresh Look at the Calculation of Tunneling Actions in Multi-Field Potentials, *JCAP* **01**, 051, [arXiv:1811.09185 \[hep-th\]](#).
- [16] J. R. Espinosa, Tunneling without Bounce, *Phys. Rev. D* **100**, 105002 (2019), [arXiv:1908.01730 \[hep-th\]](#).
- [17] J. R. Espinosa, R. Jinno, and T. Konstandin, Tunneling potential actions from canonical transformations, *JCAP* **02**, 021, [arXiv:2209.03293 \[hep-th\]](#).
- [18] E. Witten, Analytic Continuation Of Chern-Simons Theory, *AMS/IP Stud. Adv. Math.* **50**, 347 (2011), [arXiv:1001.2933 \[hep-th\]](#).
- [19] Y. Tanizaki and T. Koike, Real-time Feynman path integral with Picard–Lefschetz theory and its applications to quantum tunneling, *Annals Phys.* **351**, 250 (2014), [arXiv:1406.2386 \[math-ph\]](#).
- [20] A. Cherman and M. Unsal, Real-Time Feynman Path Integral Realization of Instantons, (2014), [arXiv:1408.0012 \[hep-th\]](#).
- [21] G. V. Dunne and M. Ünsal, What is QFT? Resurgent trans-series, Lefschetz thimbles, and new exact saddles, *PoS LATTICE2015*, 010 (2016), [arXiv:1511.05977 \[hep-lat\]](#).
- [22] S. F. Bramberger, G. Lavrelashvili, and J.-L. Lehners, Quantum tunneling from paths in complex time, *Phys. Rev. D* **94**, 064032 (2016), [arXiv:1605.02751 \[hep-th\]](#).
- [23] F. Michel, Parametrized Path Approach to Vacuum Decay, *Phys. Rev. D* **101**, 045021 (2020), [arXiv:1911.12765 \[quant-ph\]](#).
- [24] Z.-G. Mou, P. M. Saffin, and A. Tranberg, Quantum tunnelling, real-time dynamics and Picard-Lefschetz thimbles, *JHEP* **11**, 135, [arXiv:1909.02488 \[hep-th\]](#).
- [25] M. P. Hertzberg and M. Yamada, Vacuum Decay in Real Time and Imaginary Time Formalisms, *Phys. Rev. D* **100**, 016011 (2019), [arXiv:1904.08565 \[hep-th\]](#).
- [26] W.-Y. Ai, B. Garbrecht, and C. Tamarit, Functional methods for false vacuum decay in real time, *JHEP* **12**, 095, [arXiv:1905.04236 \[hep-th\]](#).
- [27] T. Hayashi, K. Kamada, N. Oshita, and J. Yokoyama, Vacuum decay in the Lorentzian path integral, *JCAP* **05** (05), 041, [arXiv:2112.09284 \[hep-th\]](#).
- [28] J. Nishimura, K. Sakai, and A. Yosprakob, A new picture of quantum tunneling in the real-time path integral from Lefschetz thimble calculations, *JHEP* **09**, 110, [arXiv:2307.11199 \[hep-th\]](#).
- [29] J. S. Langer, Theory of the condensation point, *Annals Phys.* **41**, 108 (1967).
- [30] J. S. Langer, Statistical theory of the decay of metastable states, *Annals Phys.* **54**, 258 (1969).
- [31] A. Bochkarev and P. de Forcrand, Nonperturbative evaluation of the diffusion rate in field theory at high temperatures, *Phys. Rev. D* **47**, 3476 (1993), [arXiv:hep-lat/9210027](#).
- [32] D. Boyanovsky and C. Aragao de Carvalho, Real time analysis of thermal activation via sphaleron transitions, *Phys. Rev. D* **48**, 5850 (1993), [arXiv:hep-ph/9306238](#).
- [33] M. Garny and T. Konstandin, On the gauge dependence of vacuum transitions at finite temperature, *JHEP* **07**, 189, [arXiv:1205.3392 \[hep-ph\]](#).
- [34] A. Ekstedt, Bubble nucleation to all orders, *JHEP* **08**, 115, [arXiv:2201.07331 \[hep-ph\]](#).
- [35] J. Hirvonen, J. Löfgren, M. J. Ramsey-Musolf, P. Schi-

- cho, and T. V. I. Tenkanen, Computing the gauge-invariant bubble nucleation rate in finite temperature effective field theory, *JHEP* **07**, 135, [arXiv:2112.08912 \[hep-ph\]](#).
- [36] J. Löfgren, M. J. Ramsey-Musolf, P. Schicho, and T. V. I. Tenkanen, Nucleation at Finite Temperature: A Gauge-Invariant Perturbative Framework, *Phys. Rev. Lett.* **130**, 251801 (2023), [arXiv:2112.05472 \[hep-ph\]](#).
- [37] O. Gould and J. Hirvonen, Effective field theory approach to thermal bubble nucleation, *Phys. Rev. D* **104**, 096015 (2021), [arXiv:2108.04377 \[hep-ph\]](#).
- [38] I. Affleck, Quantum Statistical Metastability, *Phys. Rev. Lett.* **46**, 388 (1981).
- [39] A. Lapedes and E. Mottola, Complex Path Integrals and Finite Temperature, *Nucl. Phys. B* **203**, 58 (1982).
- [40] J. Khoury and T. Steingasser, Gauge hierarchy from electroweak vacuum metastability, *Phys. Rev. D* **105**, 055031 (2022), [arXiv:2108.09315 \[hep-ph\]](#).
- [41] A. Shkerin and S. Sibiryakov, Black hole induced false vacuum decay from first principles, *JHEP* **11**, 197, [arXiv:2105.09331 \[hep-th\]](#).
- [42] J. Q. Liang and H. J. W. Muller-Kirsten, Nonvacuum bounces and quantum tunneling at finite energy, *Phys. Rev. D* **50**, 6519 (1994).
- [43] M. E. Carrington, The Effective potential at finite temperature in the Standard Model, *Phys. Rev. D* **45**, 2933 (1992).
- [44] K. Kajantie, M. Laine, K. Rummukainen, and M. E. Shaposhnikov, Generic rules for high temperature dimensional reduction and their application to the standard model, *Nucl. Phys. B* **458**, 90 (1996), [arXiv:hep-ph/9508379](#).
- [45] A. Salvio, A. Strumia, N. Tetradis, and A. Urbano, On gravitational and thermal corrections to vacuum decay, *JHEP* **09**, 054, [arXiv:1608.02555 \[hep-ph\]](#).
- [46] I. G. Moss, D. J. Toms, and W. A. Wright, The Effective Action at Finite Temperature, *Phys. Rev. D* **46**, 1671 (1992).
- [47] D. Bodeker, W. Buchmuller, Z. Fodor, and T. Helbig, Aspects of the cosmological electroweak phase transition, *Nucl. Phys. B* **423**, 171 (1994), [arXiv:hep-ph/9311346](#).
- [48] M. Gleiser, G. C. Marques, and R. O. Ramos, On the evaluation of thermal corrections to false vacuum decay rates, *Phys. Rev. D* **48**, 1571 (1993), [arXiv:hep-ph/9304234](#).
- [49] E. M. Chudnovsky, Phase transitions in the problem of the decay of a metastable state, *Phys. Rev. A* **46**, 8011 (1992).
- [50] T. Steingasser and D. I. Kaiser, Higgs Criticality beyond the Standard Model, (2023), [arXiv:2307.10361 \[hep-ph\]](#).